Phase transition in finite density and temperature lattice QCD *

WANG Rui(王睿)[1;1)] CHEN Ying(陈莹)[2,3] GONG Ming(宫明)[2] LIU Chuan(刘川)[4,8] LIU Yu-Bin(刘玉斌)[1]
LIU Zhao-Feng(刘朝峰)[2] MA Jian-Ping(马建平)[5] MENG Xiang-Fei(孟祥飞)[6] ZHANG Jian-Bo(张剑波)[7]
(CLQCD collaboration)

[1] School of Physics, Nankai University, Tianjin 300071, China
[2] Institute of High Energy Physics, Chinese Academy of Sciences, Beijing 100049, China
[3] Theoretical Center for Science Facilities, Chinese Academy of Sciences, Beijing 100049, China
[4] School of Physics and Center for High Energy Physics, Peking University, Beijing 100871, China
[5] Insititute of Theoretical Physics, Chinese Academy of Sciences, Beijing 100080, China
[6] National Supercomputer Center in Tianjin, Tianjin 300457, China
[7] Department of Physics, Zhejiang University, Hangzhou 310027, China
[8] Collaborative Innovation Center of Quantum Matter, Beijing 100871, China

Abstract: We investigate the behavior of the chiral condensate in lattice QCD at finite temperature and finite chemical potential. The study was done using two flavors of light quarks and with a series of β and ma at the lattice size $24\times12^2\times6$. The calculation was done in the Taylor expansion formalism. We are able to calculate the first and second order derivatives of $\langle\bar{\psi}\psi\rangle$ in both isoscalar and isovector channels. With the first derivatives being small, we find that the second derivatives are sizable close to the phase transition and that the magnitude of $\bar{\psi}\psi$ decreases under the influence of finite chemical potential in both channels.

Key words: lattice QCD, numerical simulation, chiral symmetry

PACS: 03.65.Ta, 03.67.Hk, 03.67.Lx **DOI:** 10.1088/1674-1137/39/6/063103

1 Introduction

Since the advent of lattice QCD in the 1970s by K. G. Wilson [1], it has been proven that the theory is extremely successful in the analysis of low-energy dynamics among mesons and baryons [2, 3]. Combined with large-scale computations on supercomputers, people have been investigating various non-perturbative qualities, such as the hadron spectrum, chiral transitions, behavior of glueballs, hadronic matrix elements, spatial momentum dependence and vector current correlation [4, 5].

However, lattice QCD also suffers from some shortcomings. For example, it violates some of the important symmetries that the continuum theory acquires and which can only be restored in the continuum limit. One of the most important symmetries is chiral symmetry. A well-known no-go theorem due to Nielson and Ninomiya [6] says that chiral symmetry has to be realized differently on the lattice. It is known that the fermion matrix of the lattice theory has to satisfy the so-called Ginsparg-Wilson relation [7]. One example in this category is the so-called overlap fermion. However, practical simulations of overlap fermions encounter other technical problems and are rather costly. A compromise to this problem is to use staggered fermions, which preserves part of the continuum chiral symmetry [8] and runs effectively on supercomputers.

In this article, using staggered quarks, we study the chiral condensate $\langle\bar{\psi}\psi\rangle$ and the relevant chiral symmetry breaking. As is well known, $\langle\bar{\psi}\psi\rangle$ is an important order parameter in the measurement of phase transition in lattice QCD [9–11]. Basically, the quantity $\langle\bar{\psi}\psi\rangle$ exhibits a fast decrease around the critical point but placidity in other places. This enables us to investigate the phase transition and chiral properties in both low temperature and QGP phases. Simulations of lattice QCD at finite density encounters another well-known long-lasting problem, the sign problem - the name is borrowed from condensed matter physics, where it also appears in the simulation of models with fermions. In this article we

Received 13 January 2015

∗ Supported by National Natural Science Foundation of China (11335001, 11105153, 11405178), Projects of International Cooperation and Exchanges NSFC (11261130311)

1) E-mail: huang7@mail.nankai.edu.cn

will follow the strategy of the Taylor expansion method [12], in which all physical quantities are expanded around μ=0.

This paper is organized as follows. In the next section, we briefly review the derivation of the derivatives for the chiral condensate. In the third part, our numerical results for the chiral condensate are presented and we will summarize and conclude in the fourth part.

2 Taylor expansion

When the chemical potential is present, the simulation encounters the infamous sign problem. However, if the chemical potential is not too large, everything can be expanded into a Taylor expansion in (μ/T). For the purpose of this letter, we need the expansion for $\langle\bar{\psi}\psi\rangle$,

$$\frac{\langle\bar{\psi}\psi\rangle(\mu)}{T^3} = \frac{\langle\bar{\psi}\psi\rangle(\mu)}{T^3}\bigg|_{\mu=0}+\Big(\frac{\mu}{T}\Big)\frac{1}{T^2}\frac{\partial\langle\bar{\psi}\psi\rangle}{\partial\mu}\bigg|_{\mu=0} +\Big(\frac{\mu}{T}\Big)^2\frac{1}{2T}\Big(\frac{\partial^2\langle\bar{\psi}\psi\rangle}{\partial\mu^2}\Big)\bigg|_{\mu=0}+O\bigg[\Big(\frac{\mu}{T}\Big)^3\bigg]. \quad (1)$$

The first order and second order responses in the above expansion can be computed using numerical simulation at vanishing chemical potential. Using this equation, we can investigate the behavior of $\langle\bar{\psi}\psi\rangle$ at a small but non-vanishing chemical potential.

The staggered quark fermion matrix is given by

$$\begin{aligned} D(U,\hat{\mu}) = {} & ma\delta_{n,m}+\frac{1}{2}\sum_{\sigma=x,y,z}\eta_\sigma(n) \\ & \times[U_{\hat{\sigma}}(n)\delta_{n+\hat{\sigma},m}-U^\dagger_{\hat{\sigma}}(n-\hat{\sigma})\delta_{n-\hat{\sigma},m}] \\ & +\frac{1}{2}\eta_t(n)[U_{\hat{t}}(n)\mathrm{e}^{\hat{\mu}}\delta_{n+\hat{t},m}-U^\dagger_{\hat{t}}(n-\hat{t}) \\ & \times\mathrm{e}^{-\hat{\mu}}\delta_{n-\hat{t},m}], \end{aligned} \quad (2)$$

where m is the bare quark mass, a is the lattice spacing and $\eta_{n,\mu}$ is a parameter which depends only on the parity. The parameter $\hat{\mu}=\mu/(N_tT)$ designates the chemical potential. It is switched on for each flavor of quark. In our simulation, we have both u and d quarks, whose chemical potentials are denoted by μ_{u} and μ_{d} respectively. The quark propagator is related to the Dirac operator $D[U;\hat{\mu}]$ in the background gauge field configuration U by:

$$g(\hat{\mu})=D(U,\hat{\mu})^{-1}. \quad (3)$$

In lattice QCD, the chiral condensate can be written as follows:

$$\langle\bar{\psi}\psi\rangle\equiv\mathrm{Re}\langle G\rangle=\bigg\langle\frac{1}{2}\mathrm{Re}\{\mathrm{Tr}[g(\hat{\mu}_{\mathrm{u}})]+\mathrm{Tr}[g(\hat{\mu}_{\mathrm{d}})]\}\bigg\rangle, \quad (4)$$

where Tr implies summing over all indices and $\langle\cdot\rangle$ indicates averaging over the gauge field ensembles.

For the observable $\langle G\rangle$, one can take the first and the second order derivatives with respect to the reduced chemical potential $\hat{\mu}\equiv\mu/T$ and obtain

$$\begin{aligned} \frac{\partial\langle G\rangle}{\partial\hat{\mu}} &= \bigg\langle\dot{G}+G\frac{\dot{\Delta}}{\Delta}\bigg\rangle \\ \frac{\partial^2\langle G\rangle}{\partial\hat{\mu}^2} &= \bigg\langle\ddot{G}+2\dot{G}\frac{\dot{\Delta}}{\Delta}\bigg\rangle+\bigg\langle G\frac{\ddot{\Delta}}{\Delta}\bigg\rangle-\langle G\rangle\bigg\langle\frac{\ddot{\Delta}}{\Delta}\bigg\rangle, \end{aligned} \quad (5)$$

where Δ is the fermion determinant given by

$$\Delta=\det(D(\hat{\mu}_{\mathrm{u}}))\det(D(\hat{\mu}_{\mathrm{d}})), \quad (6)$$

and a dot indicates the derivative with respect to $\hat{\mu}$.

It is interesting to investigate the response of the chiral condensate to both the isoscalar chemical potential (the traditional finite density case) and its isovector counterpart (the finite isospin density case). For the isoscalar we set

$$\hat{\mu}_{\mathrm{S}}=\hat{\mu}_{\mathrm{u}}=\hat{\mu}_{\mathrm{d}}, \quad (7)$$

while for the isovector case we choose

$$\hat{\mu}_{\mathrm{V}}=\hat{\mu}_{\mathrm{u}}=-\hat{\mu}_{\mathrm{d}}. \quad (8)$$

We will call these two cases the isoscalar and isovector channels in the following by calculating the corresponding derivatives of G with respect to the corresponding chemical potential. It is known that the first order derivative for both the isoscalar case and the isovector case are zero, so the second order derivatives become crucial in our calculation.

3 Numerical simulation and results

The conventional Wilson plaquette action is used, which is characterized by the parameter β. The gauge field configurations are generated using the conventional R-algorithm for Hybrid Monte Carlo with molecular dynamics step δ=0.01 and trajectory length of 50. The size of the lattices are all $24\times12^2\times6$ and for each parameter set, 600 gauge field configurations are obtained. By scanning the temperature dependence of the Polyakov loop the ratio T/T_{c} can be determined. This information, together with other simulation parameters, is summarized in Table 1.

We have calculated the value of $\langle\bar{\psi}\psi\rangle$ and its second order derivatives for both $\hat{\mu}_{\mathrm{S}}$ and $\hat{\mu}_{\mathrm{V}}$ for all our data sets and the results are listed in Table 2. The temperature dependence of the second order derivatives of $\langle\bar{\psi}\psi\rangle$ with respect to $\hat{\mu}_{\mathrm{S}}$ and $\hat{\mu}_{\mathrm{V}}$ are illustrated in Fig. 1 for ma=0.020.

It is seen from Fig. 1 that the second order derivatives in both isoscalar and isovector channels share some common features. They are both negative but the absolute value is very small when away from the critical point. Close to the critical point, both increase substantially.

Now it is possible to consider the behavior of $\langle\bar{\psi}\psi\rangle$

Table 1. Simulation parameters used in this study. All lattices are of size $24^2\times12\times6$ and $N_{\rm conf}$ stands for the number of configurations.

ma	β	$N_{\rm conf}$	$T/T_{\rm c}$
0.020	5.292	600	0.90
0.020	5.327	600	0.95
0.020	5.347	600	0.98
0.020	5.373	600	1.02
0.020	5.392	600	1.05
0.020	5.422	600	1.10
0.015	5.317	600	0.95
0.015	5.337	600	0.98
0.015	5.363	600	1.02
0.015	5.382	600	1.05
0.012	5.327	600	0.95
0.012	5.347	600	0.98
0.012	5.373	600	1.02
0.012	5.392	600	1.05

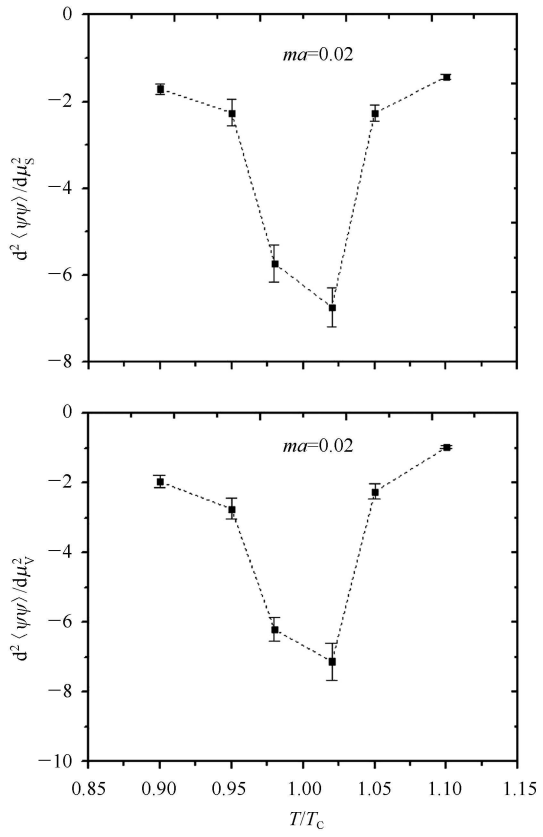

Fig. 1. Second order derivatives of $\langle\bar\psi\psi\rangle$ at ma=0.020.

with chemical potential and temperature in the critical region for both channels. We omit the first order derivatives, since they vanish, and only consider the second order derivatives. Using the data listed in Table 2, we obtain the following expansion near $\beta_{\rm c}$. For instance, slightly below $T_{\rm c}$ at β=5.347 and ma=0.020, we obtain:

$$\frac{\langle\bar\psi\psi\rangle(\mu_{\rm S})}{T^3} = 70.2(6.0)-17.2(1.3)\left(\frac{\mu_{\rm S}}{T}\right)^2 +O\left[\left(\frac{\mu_{\rm S}}{T}\right)^3\right], \quad (9)$$

$$\frac{\langle\bar\psi\psi\rangle(\mu_{\rm V})}{T^3} = 70.2(6.0)-18.6(1.0)\left(\frac{\mu_{\rm V}}{T}\right)^2 +O\left[\left(\frac{\mu_{\rm V}}{T}\right)^3\right]. \quad (10)$$

As we can see, the derivative corrections are quite substantial in the critical region. Thus, the effect of the chemical potential makes $\beta_{\rm c}$ drop from its original value at $\mu=0$. At an even lower temperature, for example, β=5.292 and ma=0.020, the data suggests

$$\frac{\langle\bar\psi\psi\rangle(\mu_{\rm S})}{T^3} = 79.2(2.7)-5.13(37)\left(\frac{\mu_{\rm S}}{T}\right)^2 +O\left[\left(\frac{\mu_{\rm S}}{T}\right)^3\right], \quad (11)$$

$$\frac{\langle\bar\psi\psi\rangle(\mu_{\rm V})}{T^3} = 79.2(2.7)-5.88(55)\left(\frac{\mu_{\rm V}}{T}\right)^2 +\left[\left(\frac{\mu_{\rm V}}{T}\right)^3\right]. \quad (12)$$

These derivative corrections are not as large as is the case in the critical region. In the phase above $T_{\rm c}$ (in the QGP phase) at β=5.422 and ma=0.020, we obtain

$$\frac{\langle\bar\psi\psi\rangle(\mu_{\rm S})}{T^3} = 25.8(1.8)-4.29(15)\left(\frac{\mu_{\rm S}}{T}\right)^2 + O\left[\left(\frac{\mu_{\rm S}}{T}\right)^3\right], \quad (13)$$

$$\frac{\langle\bar\psi\psi\rangle(\mu_{\rm V})}{T^3} = 25.8(1.8)-2.95(12)\left(\frac{\mu_{\rm V}}{T}\right)^2 + O\left[\left(\frac{\mu_{\rm V}}{T}\right)^3\right]. \quad (14)$$

Table 2. The values of $\langle\bar\psi\psi\rangle$ and its second order derivatives in the isoscalar and isovector channels.

ma	β	$\langle\bar\psi\psi\rangle$	$\frac{\partial^2\langle\bar\psi\psi\rangle}{\partial\hat\mu_{\rm S}^2}$	$\frac{\partial^2\langle\bar\psi\psi\rangle}{\partial\hat\mu_{\rm V}^2}$
0.020	5.292	0.367(13)	−1.71(12)	−1.96(18)
0.020	5.327	0.351(13)	−2.26(31)	−2.75(30)
0.020	5.347	0.325(28)	−5.73(42)	−6.21(34)
0.020	5.373	0.138(24)	−6.73(45)	−7.12(53)
0.020	5.392	0.129(10)	−2.27(19)	−2.25(22)
0.020	5.422	0.119(8)	−1.43(5)	−0.98(4)
0.015	5.317	0.367(26)	−2.81(31)	−2.79(29)
0.015	5.337	0.335(33)	−7.07(59)	−6.55(56)
0.015	5.363	0.144(28)	−6.39(36)	−5.92(34)
0.015	5.382	0.123(8)	−2.13(20)	−2.62(24)
0.012	5.327	0.377(21)	−2.97(26)	−2.83(28)
0.012	5.347	0.347(34)	−6.08(41)	−6.17(45)
0.012	5.373	0.148(28)	−5.68(35)	−5.67(32)
0.012	5.392	0.126(7)	−2.55(23)	−1.84(17)

We can now plot the results for the chiral condensate at small chemical potential in both the isoscalar and the isovector channels. This is illustrated in Fig. 2.

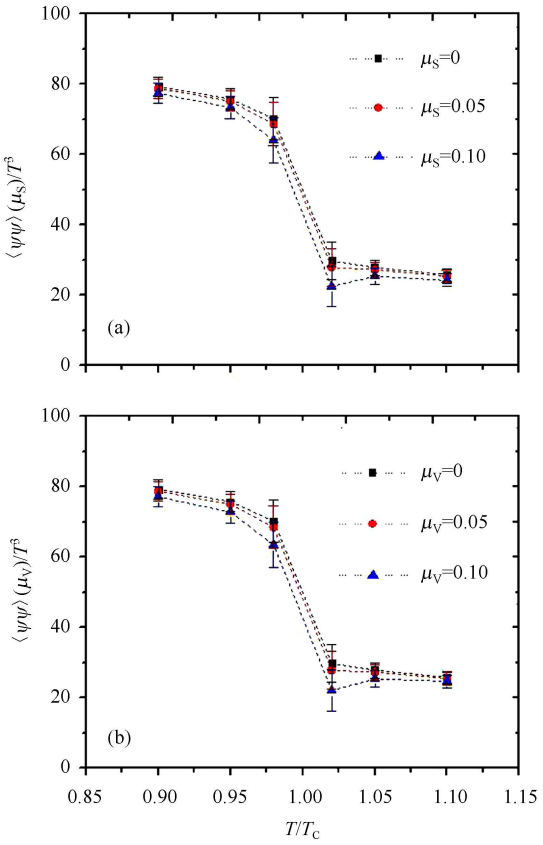

Fig. 2. Behavior of $\langle\bar{\psi}\psi\rangle$ at finite isoscalar chemical potential (a) and isovector potential (b).

In this figure, we include the behavior of $\langle\bar{\psi}\psi\rangle$ for the chemical potential $\hat{\mu}_{\rm S,V}=0.05$ and $\hat{\mu}_{\rm S,V}=0.10$. Since the second order derivatives are all negative, we find the critical temperature tends to decrease under the influence of $\hat{\mu}_{\rm S,V}$. Thus, in the low temperature phase, turning on the chemical potential brings the system closer to the phase transition where chiral symmetry is restored and decreases the magnitude of the chiral condensate. In the high temperature phase, however, since chiral symmetry is already restored, the responses of the chiral condensate to the isoscalar and isovector chemical potential are relatively small.

4 Conclusions

In this work, we have studied the response of the chiral condensate $\langle\bar{\psi}\psi\rangle$ to the chemical potentials using the Taylor expansion method. The quantity is expanded around $\mu=0$ and the second derivatives of $\langle\bar{\psi}\psi\rangle$ with respect to both $\mu_{\rm S}$ and $\mu_{\rm V}$ are obtained. As is seen, though the first order derivatives are small, the second order responses are sizable and exhibit several unique features. The behavior of the responses for the $\langle\bar{\psi}\psi\rangle$ is closely related to chiral restoration. For both isoscalar and isovector channels, we find that the critical temperature decreases with the influence of both chemical potentials, and the magnitude of $\langle\bar{\psi}\psi\rangle$ tends to decrease under finite chemical potential.

The numerical calculations were performed on the TianHe-1A supercomputer at the National Supercomputer Center in Tianjin.

References

1 Wilson K G. Phys. Rev. D, 1974, **10**: 2445
2 Martin A, Richard J M et al. Phys. Lett. B, 1995, **355**: 345
3 Alexandrou C, Borrelli A et al. Phys. Lett. B, 1994, **337**: 340
4 Tripolt R A, Smekal L V et al. Phys. Rev. D, 2014, **90**: 074031
5 DING Heng-Tong, Francis A et al. Phys. Rev. D, 2011, **83**: 034504
6 Nielson H B, Ninomiya M et al. Nucl. Phys. B, 1981, **193**: 173
7 Ginparg P H, Wilson K G et al. Phys. Rev. D, 1982, **25**: 2649
8 Maarten F L Golterman. Nucl. Phys. B, 1986, **278**: 417
9 Bali G S, Bruckmann F et al. JHEP, 2012, **1202**: 044
10 GAO Jian-Hua, LIANG Zuo-Tang et al. Phys. Rev. Lett, 2012, **109**: 232301
11 YU Lang, LIU Hao et al. Phys. Rev. D, 2014, **90**: 074009
12 Choe S, Forcrand P D et al. Phys. Rev. D, 2002, **65**: 054501